

**MOLECULAR MODELING STUDY OF SOME DIPEPTIDYL PEPTIDASE IV (DPP-IV)  
INHIBITORS AS ANTIDIABETIC AGENTS**Steffy Mary Chandy\*, Sudha Vengurlekar<sup>1</sup> and S. C. Chaturvedi<sup>1</sup>\*<sup>1</sup>Sri Aurobindo Institute of Pharmacy, Indore (M.P.).

\*Corresponding Author: Steffy Mary Chandy

Sri Aurobindo Institute of Pharmacy, Indore (M.P.).

Article Received on 16/12/2018

Article Revised on 06/01/2019

Article Accepted on 27/01/2019

**ABSTRACT**

Type II diabetes is establishing itself as an epidemic of the 21<sup>st</sup> century and is a severe and increasingly prevalent disease. The present study successfully applied pharmacophore mapping, 3D-QSAR and molecular docking analysis to characterize a set of synthesized DPP-IV inhibitors. The selected series of imidazoquinoline derivatives included 47 compounds out of which 38 compounds were put in training set and remaining 9 compound were put in test set on the basis of diversity using the SYBYL X 2.1.1 software. The pharmacophore models were derived using GALAHAD module of SYBYL X 2.1.1 software. The optimal pharmacophore model contains nine pharmacophore features. The models include four hydrophobes, three hydrogen bond acceptors and two positive nitrogen centres. Successful CoMFA models were generated from imidazoquinoline derivatives which displayed a cross-validated correlation coefficient ( $Q^2$ ) of 0.526 and a non-cross related coefficient ( $R^2$ ) of 0.946. Moreover the contour maps derived from CoMFA models provided enough information to understand the SAR and to identify the structural features influencing DPP-IV inhibitory activity. The docking studies of the eight designed compounds were performed using the SURFLEX DOCK module of SYBYL X 2.1.1 software. The binding mode of designed compounds at the active site of DPP-IV enzyme (PDB ID. 4DSA) was explored and hydrogen-bonding interactions were observed between the inhibitor and the target.

**KEYWORDS:** Type II diabetes, DPP-IV inhibitors, SYBYL X 2.1.1 software, GALAHAD, SURFLEX DOCK, imidazoquinoline derivatives.

**1. INTRODUCTION**

**Diabetes**, also called as **diabetes mellitus**, is a group of metabolic diseases which is characterized by high blood glucose level. It may be due to insufficient production of insulin, or inability of body to utilize the produced insulin or both.<sup>[1]</sup> Type II diabetes is establishing itself as an epidemic of the 21<sup>st</sup> century and is a severe and increasingly prevalent disease.<sup>[2]</sup>

Type II diabetes is a major metabolic disorder affecting approximately 194 million people worldwide. This number is estimated to reach 366 million by 2030.<sup>[3]</sup> Currently used antidiabetic agents, such as PPARc agonists, sulphonylurea derivatives, and biguanide and  $\alpha$ -glucosidase inhibitors, produce beneficial effects on type II diabetes by effectively increasing insulin secretion or decreasing glucose absorption.<sup>[4]</sup>

However, these agents are known to be associated with a number of side effects, including hypoglycemia, weight gain, gastrointestinal disorders, and lactic acidosis, all of which are known to decrease quality of life for type II diabetes patients. Under these circumstances, intensive efforts have been made to find better and safer oral drugs for type II diabetes.<sup>[4]</sup>

Glucagon-like peptide-1 (GLP-1) is secreted from the gut in response to glucose absorption following meal ingestion and stimulates insulin secretion from  $\beta$ -cells of the pancreas, thereby contributing to maintenance of postmeal glycemic control. As GLP-1 in plasma is rapidly degraded by the serine protease dipeptidyl peptidase IV (DPP-IV), inhibition of DPP-IV is emerging as a promising approach for treatment of T2D with low risk of hypoglycemia.<sup>[5]</sup>

Actually, clinical proof of concept has already been established with DPP-IV inhibitors, which proved to be more efficient and safer than conventional antidiabetic agents. Based on these clinical findings, a number of DPP-4 inhibitors, including Sitagliptin, Vildagliptin, Saxagliptin, Alogliptin and Linagliptin have already been approved as new valuable agents for treatment of T2D.<sup>[6-8]</sup>

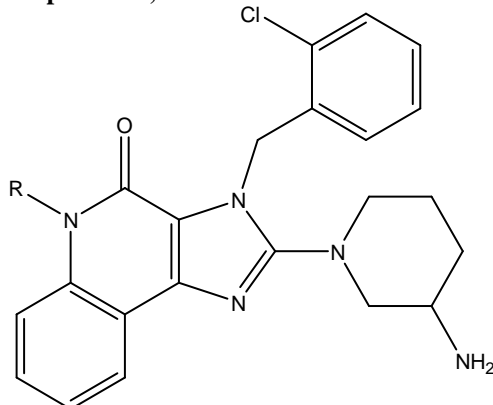
**2. MATERIALS AND METHOD****A. Dataset**

The molecular structures and biological data used in the molecular modeling study consisted of quinoline derivatives as DPP-IV inhibitors.<sup>[9]</sup> Molecules in this series have basic structure 3H-imidazo [4, 5-c]

quinoline-4(5H)-ones. Structure and biological activity of values for DPP-IV inhibitors for all molecules are given in the Table 1, 2 and 3. The compounds were

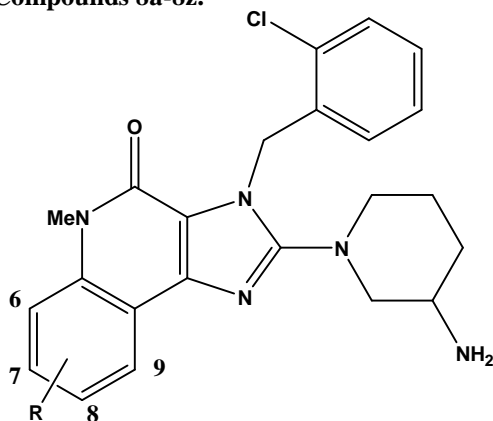
divided into test and training set on the basis of diversity of compounds.

**Table 1: IC<sub>50</sub> and pIC<sub>50</sub> Values of Compounds 2,2a-2d.**<sup>[9]</sup>



S. NO	Compound	R	IC <sub>50</sub> nm	pIC <sub>50</sub>
1	2	H	418	6.3788
2	2a	Me	103	6.9872
3	2b	Et	400	6.3979
4	2c	nPr	3400	5.4685
5	2d	Bn	10000	5

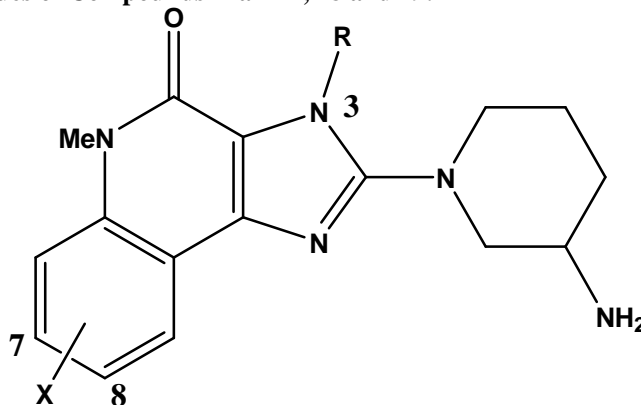
**Table 2: IC<sub>50</sub> and pIC<sub>50</sub> Values of Compounds 8a-8z.**<sup>[9]</sup>



S. NO	Compound	R	IC <sub>50</sub> nm	pIC <sub>50</sub>
1	8a	6-OMe	660	6.1805
2	8b	6-CO <sub>2</sub> Me	271	6.567
3	8c	6-CO <sub>2</sub> H	72	7.1427
4	8d	7-F	66	7.1805
5	8e	7-Ph	72	7.1427
6	8f	7-Me	340	6.4685
7	8g	7-OMe	66	7.1805
8	8h	7-CH <sub>2</sub> OMe	17	7.7696
9	8i	7-CH <sub>2</sub> OH	22	7.6576
10	8j	7-CO <sub>2</sub> Me	16	7.7959
11	8k	7-CONH <sub>2</sub>	12	7.9208
12	8l	7-CONMe <sub>2</sub>	10	8
13	8m	7-CN	6.3	8.2007
14	8n	7-CO <sub>2</sub> H	1.6	8.7959
15	8o	7-CH <sub>2</sub> CO <sub>2</sub> H	3.8	8.4202
16	8p	8-OMe	90	7.0458
17	8q	8-Me	94	7.0269
18	8r	8-F	56	7.2518

19	8s	8-OCHF <sub>2</sub>	60	7.2218
20	8t	8-CO <sub>2</sub> Me	21	7.677
21	8u	8-CONH <sub>2</sub>	14	7.8539
22	8v	8-CONMe <sub>2</sub>	13	7.8861
23	8w	8-CO <sub>2</sub> H	5.8	8.2366
24	8x	8-CH <sub>2</sub> CO <sub>2</sub> H	3.5	8.4559
25	8y	9-CO <sub>2</sub> H	54	7.2676
26	8z	9-CH <sub>2</sub> CO <sub>2</sub> H	17	7.7696

**Table 3: IC<sub>50</sub> and pIC<sub>50</sub> Values of Compounds 24a-24n, 28 and 29.<sup>[9]</sup>**



S. NO	Compound	X	R	IC <sub>50</sub> nm	pIC <sub>50</sub>
1	24a	8-CO <sub>2</sub> H	Benzyl	64	7.1938
2	24b	8-CO <sub>2</sub> H	2-Methylbenzyl	11	7.9586
3	24c	8-CO <sub>2</sub> H	2-Methoxybenzyl	38	7.4202
4	24d	8-CO <sub>2</sub> H	2-Fluorobenzyl	160	6.7959
5	24e	8-CO <sub>2</sub> H	3-Chlorobenzyl	110	6.9586
6	24f	8-CO <sub>2</sub> H	4-Chlorobenzyl	10000	5
7	24g	8-CO <sub>2</sub> H	3-Methoxybenzyl	150	6.8239
8	24h	8-CO <sub>2</sub> H	4-Methoxybenzyl	6900	5.1612
9	24i	8-CO <sub>2</sub> H	2-Chlorophenethyl	3500	5.4559
10	24j	8-CO <sub>2</sub> H	Cyclohexylmethyl	8900	5.0506
11	24k	8-CO <sub>2</sub> H	Methylbut-2-enyl	51	7.2924
12	24l	8-CO <sub>2</sub> H	But-2-ynyl	90	7.0458
13	24m	8-CO <sub>2</sub> H	2,5-Dichlorobenzyl	25	7.6021
14	24n	8-CO <sub>2</sub> H	2-Chloro-5-fluorobenzyl	4.8	8.3188
15	28	7-CO <sub>2</sub> H	2-Chloro-5-fluorobenzyl	0.48	9.3188
16	29	7-CO <sub>2</sub> H	5-Fluoro-2-methylbenzyl	0.55	9.2596

### B. Software

The chemical structures of all the molecules were sketched using Chem Draw Ultra 7.0. All computational studies were performed using Sybyl X 2.1.1 software.<sup>[10]</sup>

### C. Pharmacophore Modeling

Genetic algorithm with linear assignment of hypermolecular alignment of datasets (GALAHAD) module of SYBYL X 2.1.1 software was used to generate the pharmacophore models. The selected series included 47 compounds out of which 38 compounds were put in training set and remaining 9 compound were put in test set on the basis of diversity using SYBYL X 2.1.1 software. All the compounds in the training set were prepared by the following procedures: bond orders of structure were checked, additions of hydrogen atoms were done and energy minimization was done using the MMFF94 force-field. GALAHAD was run for 50

generations with a population size of 100. The CoMFA molecular modelling studies were performed using TRIPOS module of SYBYL-X 2.1.1 software. Five pharmacophore models were generated from 9 compounds in test set.

### D. CoMFA

The Comparative molecular field analysis molecular modelling studies were performed using TRIPOS module of SYBYL-X 2.1.1 software.<sup>[10]</sup> The steric and electrostatic field effects were calculated using the TRIPOS force field. The CoMFA models were developed using 38 compounds as training set, and validated using 9 compounds as test set (Table 7 and 8). The compound set was randomly divided into a training set and a test set. The range of pIC<sub>50</sub> values for both the training and test set spans at least three orders of

magnitude, and in addition the biological activity values are well distributed over the entire range.

Five different kinds of partial charges are considered:

- (1) Gasteige charges
- (2) Gast-Huck charges
- (3) Delre charges
- (4) Pullman charges
- (5) Formal charges and
- (6) MMFF94 charges

### E. Molecular Docking

The novel compounds designed were docked using SURFLEX DOCK module of SYBYL X 2.1.1 software<sup>[10]</sup> to predict their DPP-IV inhibitory activity. The crystal structure of DPP-IV receptor (3.28 Å, 4DSA.pdb) shown in fig. 1 was selected as the docking template. The ligand 4-[[[(2R)-2-amino-3-(2,4,5-trifluorophenyl)propyl]sulfamoyl] amino) methyl] benzenesulfonamide (C1) was extracted, crystallographic water molecules in the structure were removed, hydrogen atoms of modeled structure were added to define the correct configuration. After extracting the binding ligand, the structure of DPP-IV receptor was used for docking and the docking score was calculated. The default parameters, as implemented in the SYBYL X-2.1.1 software, were used.

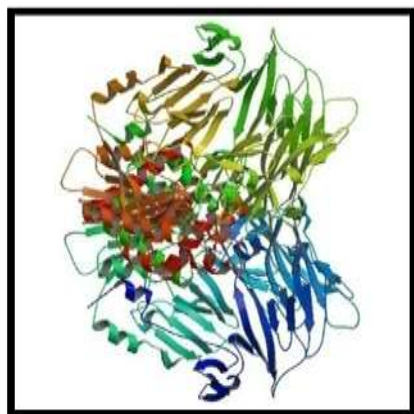


**Figure 1: Biological Assembly Image for 4DSA (Crystal Structure of DPP-IV with Compound C1).**

## 3. RESULT AND DISCUSSION

### A. Pharmacophore Modeling

A pharmacophore is an ensemble of steric and electronic features that are necessary for a ligand to provide optimal molecular interaction with a specific biological target and to trigger (or block) its biological response.<sup>[11]</sup>

In principle, a pharmacophore model could be simulated by deriving the common essential structural characteristics responsible for their bioactivities based on molecular alignment of a known set of bioactive ligands. The pharmacophore model generated could then be applied to virtually screen a compound database for chemically diverse molecules that shared similar

structural features and their relative spatial arrangement defined in the pharmacophore model.

The number of hits column indicates that all models hit all ligands in the dataset and each of them has seven features in it. Pareto rank indicates that no model is more or less superior to each another.<sup>[12]</sup>

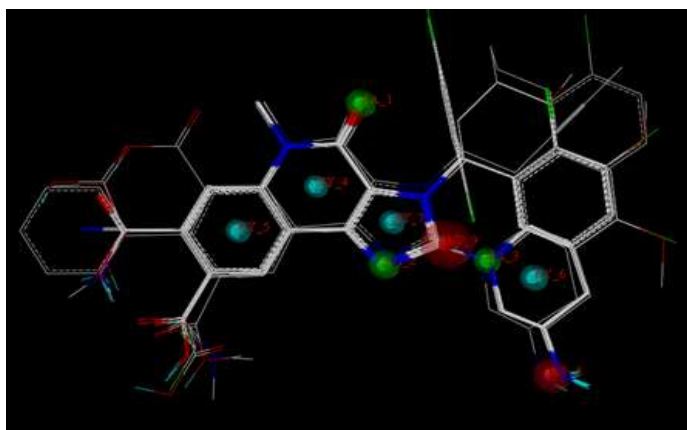
A series of imidzoquinoline derivatives were taken from the literature for the pharmacophore studies. The selected series of imidazoquinoline derivatives included 47 compounds out of which 38 compounds were put in training set and remaining 9 compound were put in test set on the basis of diversity using the SYBYL X 2.1.1 software. Results are given in Fig. 34 and 35 for each GALAHAD generated pharmacophore model for training set and test set compounds.

The energy term of computer-generate pharmacophore model 1 was 49.54kcal mol, which designates the total energy (using the Tripos force field) of all molecules. Meanwhile, the values of sterics, H-bond and MOL\_QRY were computed as 4564.1001, 889.5 and 170.21 respectively, in Model 1. In the GALAHAD algorithm, sterics is defined as the overall steric similarity among ligand conformers, H-bond as the overall pharmacophoric similarity among ligand conformers, and MOL\_QRY represents the agreement between the query and the pharmacophoric features of the target ligands as a group.<sup>[12]</sup>

In general, a good pharmacophore model should have a maximized steric consensus, maximized pharmacophore consensus, and minimized energy. As shown in Table 9, the pharmacophore Model 1 had the lowest value for energy, in comparison to the other nine models. Model 1 was therefore selected as the final pharmacophore model for imidazoquinoline derivatives.

**Table 9: The Parameter Values for Each Pharmacophore Model of Training Set.**

S.n	Name	Specificity	Hits	Feats	Pareto	Energy	Sterics	H-bond	Mol Qry
1	1	2.86	0	9	0	49.54	4564.1001	889.5	170.21
2	2	2.859	0	9	0	6724868928	4734.3999	883.9	192.54
3	3	2.86	0	9	0	56.92	4808.2998	838.2	180.89
4	4	2.859	0	9	0	435172.406	4712.1001	880.5	181.81
5	5	2.861	0	9	0	1066860224	4806.2998	871.4	176.76
6	6	2.861	0	9	0	1150482432	4739.2998	885.6	159.1
7	7	2.86	0	9	0	52.84	4719.1001	856.2	168.95
8	8	2.859	0	9	0	3157616128	4746.1001	885.1	152.64
9	9	2.859	0	9	0	52.49	4662.1001	840.8	144.13
10	10	2.859	0	9	0	52.34	4672.7002	878.7	165.53

**Figure 2: Pharmacophore model 1 and molecular alignment of training set compounds (Table 7).**

In general, a good pharmacophore model should have a maximized steric consensus, maximized pharmacophore consensus, and minimized energy. As shown in Table 9, the pharmacophore Model 1 had the lowest value for energy, in comparison to the other nine models. Model 1 was therefore selected as the final pharmacophore model for imidazoquinoline derivatives. As illustrated in Fig. 2, the GALAHAD-generated pharmacophore Model 1 for most active compound in the series (compound 28) contained three H-bond acceptor features (AA\_1, AA\_2

and AA\_3), four hydrophobic centres (HY\_4, HY\_5, HY\_6 and HY\_7) and two positive nitrogen centres (NP\_8 and NP\_9). For all the 9 compounds in the test set GALAHAD was run for 50 generations with a population size of 55. Five pharmacophore models were generated from 9 compounds in test set. Table 10 shows the predictable results for each model. Model 003 with the lowest value of energy (63.43), was considered to be the best model.

**Table 10: The Parameter Values for Each Pharmacophore Model of Test Set.**

S.n	Name	Specificity	Hits	Feats	Pareto	Energy	Sterics	H-bond	Mol Qry
1	1	2.858	0	9	0	101014	5255	907.9	167.07
2	2	2.858	0	9	0	91	4707.2002	864.2	170.96
3	3	2.858	0	9	0	63.43	5147.2002	859.2	153.48
4	4	2.858	0	9	0	863.54	5084.8999	902.6	153.26
5	5	2.858	0	9	0	1898.9399	4912.3999	896.1	155.61

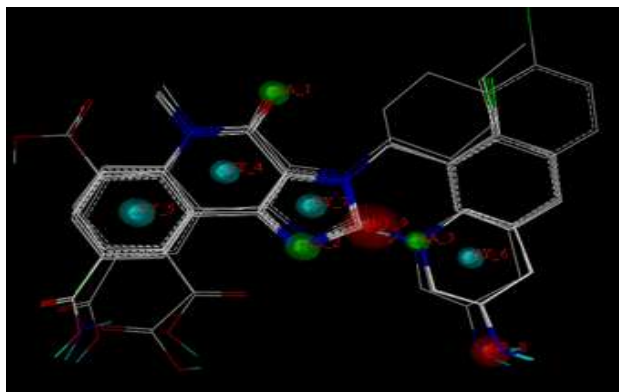


**Figure 3: Pharmacophore model 3 and molecular alignment of test set compounds (Table 8).**

Generated pharmacophore model shown in fig. 3 contained three H-bond acceptor features (green), four hydrophobic features (cyan) and two positive nitrogen centres (red).

### B. CoMFA

CoMFA models of 47 imidazoquinoline analogues were divided into training set of 38 molecules and test set of 9 molecules the basis of diversity using the SYBYL X 2.1.1 software. Predictive power of resulting model was evaluated using a test set of 9 molecules. The statistical parameters associated with CoMFA models of this series are listed in table 11, 12 and 13. A 3D QSAR model is considered statistically significant if its  $Q^2$  value is above 0.3 although a  $Q^2$  value above 0.4 to 0.5 is naturally preferable.  $Q^2$  value for all the charges were above 0.4

except for Gast-Huck charge, which was excluded. Formal charge with a  $Q^2$  value of 0.526 was considered the best model. The CoMFA models derived from the 38 training compounds for formal charges from using both steric and electrostatic fields gave a cross-validated correlation coefficient ( $Q^2$ ) of 0.526. A non-cross related coefficient ( $R^2$ ) of 0.946 with a low standard error estimate (SEE) of 0.265618 was obtained. The contributions of steric and electrostatic fields were 66.76% and 0% respectively. Whereas cross-validated correlation coefficient ( $Q^2$ ), non-cross related coefficient ( $R^2$ ) and standard error estimate (SEE) for MMFF94 charge was found to be 0.494, 0.948 and 0.27334. The contributions of steric and electrostatic fields were 18.47% and 12.08% respectively.

**Table 11: Summary of CoMFA analyses results.**

S.no	Model name	$Q^2$	$R^2$	Std. error	Steric contribution %		Electrostatic contribution %	
					Steric bulk desirable	Steric bulk undesirable	Positive charge desirable	Negative charge desirable
1	K2	0.473	0.898	0.372548	12.20	6.92	29.02	31.83
2	K4	0.266	0.484	0.801739	-	-	-	-
3	K6	0.486	0.909	0.351	20.52	10.46	39.29	9.70
4	K8	0.461	0.951	0.265618	23.15	31.31	4.78	20.75
5	K10	0.526	0.946	0.265618	66.76	13.23	0	0
6	K12	0.494	0.948	0.27334	18.47	28.39	12.08	20.23

\*K2- Gasteiger charge, K4-Gast Huck charge, K6- Delre charge, K8-Pullman charge, K10-Formal charge, K12-MMFF94.

**Table 12: The experimental  $pIC_{50}$  values and predicted  $pIC_{50}$  values of the training set compounds.**

S.no	Comp. name	Experimental $pIC_{50}$	Predicted $pIC_{50}$				
			Gasteiger	Delre	Pullman	Formal	MMFF94
1	2	6.3788	6.6093	6.5288	6.5454	6.1754	6.5583
2	2a	6.9872	6.6296	6.5915	6.6789	6.776	6.7009
3	2b	6.3979	6.2592	6.1	6.1313	6.2872	6.1376
4	2c	5.4685	5.941	5.7176	5.5457	5.4107	5.5405
5	2d	5	5.2887	5.2646	4.973	5.1423	4.9765
6	8c	7.1427	7.2841	7.4114	7.2926	7.5226	7.3274
7	8d	7.1805	7.1453	7.1009	7.1072	6.8912	7.1027
8	8e	7.1427	7.1591	7.2509	7.2354	7.1907	7.2637
9	8f	6.4685	6.9023	7.0293	6.8792	7.068	6.9793
10	8g	7.1805	7.3104	7.5763	7.3132	7.4429	7.3432
11	8h	7.7696	7.5993	7.4603	7.761	7.8485	7.717
12	8i	7.6576	7.5839	7.7689	7.5477	7.2464	7.5102

13	8j	7.7959	7.9971	7.8971	7.8947	7.7758	7.8556
14	8k	7.9208	8.1443	7.8463	8.1303	8.0655	8.098
15	8l	8	7.7949	7.9989	7.5023	8.0583	7.771
16	8m	8.2007	7.6003	7.5092	8.0953	8.0788	8.019
17	8n	8.7959	8.5679	8.4846	8.7633	8.4654	8.8376
18	8o	8.4202	8.1521	8.3531	8.3234	8.2317	8.3104
19	8p	7.0458	6.7708	7.1085	6.9162	7.0255	6.8429
20	8q	7.0269	6.9014	7.0438	7.0768	7.4029	7.6523
21	8s	7.2218	7.3711	7.4035	7.138	7.3442	7.0863
22	8t	7.677	7.665	7.7693	7.5665	7.5795	7.5899
23	8v	7.8861	7.7737	8.0262	7.7475	7.9861	7.7625
24	8w	8.2366	7.4372	7.5786	7.537	7.6041	7.6147
25	8x	8.4559	8.7956	8.5106	8.5585	8.32	8.4759
26	24b	7.9586	7.1607	7.086	7.4695	7.9202	7.501
27	24c	7.4202	7.7069	7.6937	7.7745	7.4107	7.7978
28	24d	6.7959	7.6057	7.563	7.4736	7.5527	7.5556
29	24e	6.9586	6.9427	6.8267	6.955	6.9448	7.0098
30	24f	5	5.803	5.2444	5.2141	5.0918	5.2595
31	24g	6.8239	6.734	6.7687	7.0808	6.6293	7.0117
32	24h	5.1612	4.7353	4.9067	4.9925	5.1046	4.9489
33	24j	5.0506	4.917	4.9367	5.0314	5.0445	5.0093
34	24l	7.0458	7.0027	7.0619	7.1154	7.0347	7.1037
35	24m	7.6021	7.8678	8.0481	7.7921	7.4803	7.7637
36	24n	8.3188	8.3087	8.4294	8.2341	8.5027	8.2084
37	28	9.3188	9.441	9.3432	9.4571	9.3648	9.428
38	29	9.2596	9.2638	8.9377	9.043	9.1524	9.0933

Table 13: The experimental  $pIC_{50}$  values and predicted  $pIC_{50}$  values of the test set compounds.

S.no	Comp. name	Experimental $pIC_{50}$	Predicted $pIC_{50}$				
			Gasteiger	Delre	Pullman	Formal	MMFF94
1	8a	6.1805	7.1108	6.832	6.7039	6.6175	6.8859
2	8b	6.567	7.6217	7.3365	7.258	6.6128	7.2733
3	8r	7.2518	6.7035	6.7385	6.6629	6.8681	6.7325
4	8u	7.8539	7.3851	7.7657	7.4406	8.0051	7.5429
5	8y	7.2676	9.9709	6.7316	6.931	6.8717	6.9806
6	8z	7.7696	7.3614	7.8775	7.2467	7.6175	7.2423
7	24a	7.1938	7.0047	6.8753	6.9705	7.0314	7.0019
8	24i	5.4559	7.0066	7.4112	7.0517	5.9344	4.2689
9	24k	7.2924	7.2924	7.2056	7.5044	7.6754	7.4358

### CoMFA Contour Maps

The results obtained from CoMFA indicate that steric and electrostatic properties play a major role in inhibition activity (Table 11, 12 and 13). The steric interactions are represented by green and yellow colored contours while electrostatic interactions are represented by red and blue colored contours. In steric field, green contour represents region where bulky substituent enhances activity, whereas yellow contour indicates region where bulky substituents decrease the activity. In case of electrostatic interactions, the blue contour represents region where electropositive groups enhance the activity, while red-colored region indicates that electronegative groups increases the activity.<sup>[12]</sup>

One of the most active compounds in the series (compound 28) is shown with CoMFA contour maps of steric and electrostatic fields in Figs. 4-8.

As shown in the CoMFA contour maps of compound 28 which is the most active compound, the green contour was favored around the benzene ring attached to quinoline indicates that bulky substituents at the X increases activity like COOH, CONH<sub>2</sub>, CN, CH<sub>2</sub>COOH, etc. Sterically unfavorable contour in yellow color were found near R in quinoline ring and around 3-amino piperidine ring. Thus bulky substituents decrease activity. Blue contour near R and quinoline ring indicates that substituents with electropositive group enhance activity. While red colour on substituent R i.e. 2-chloro-5-fluorobenzyl indicates that electronegative group at this position enhances activity.

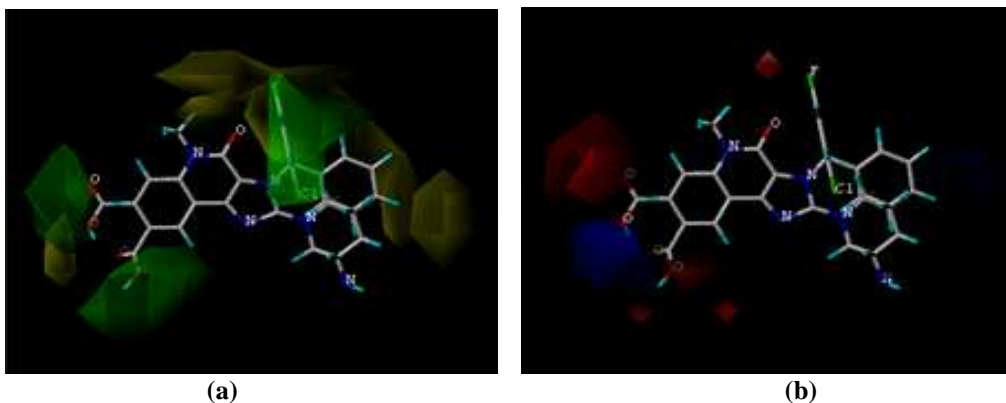


Figure 4: CoMFA contour maps for Gasteiger charge (of Compound 28, Table 7)

(a) Steric contributions, (b) Electrostatic contributions.

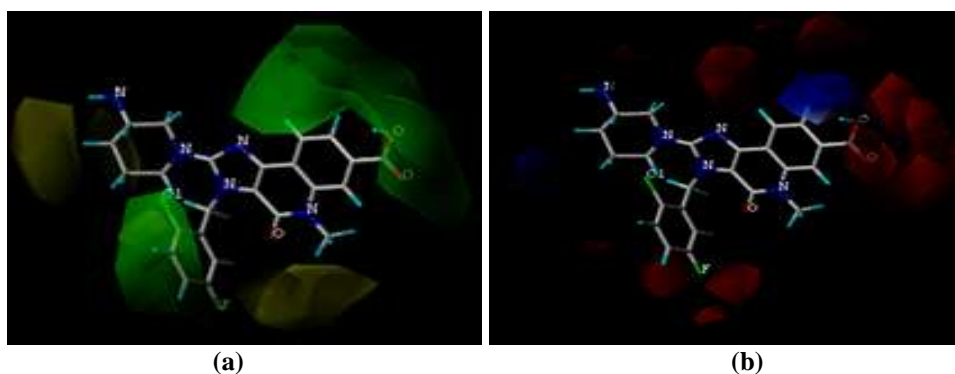


Figure 5: CoMFA contour maps for Delre charge (of Compound 28, Table 7)

(a) Steric contributions, (b) Electrostatic contributions.

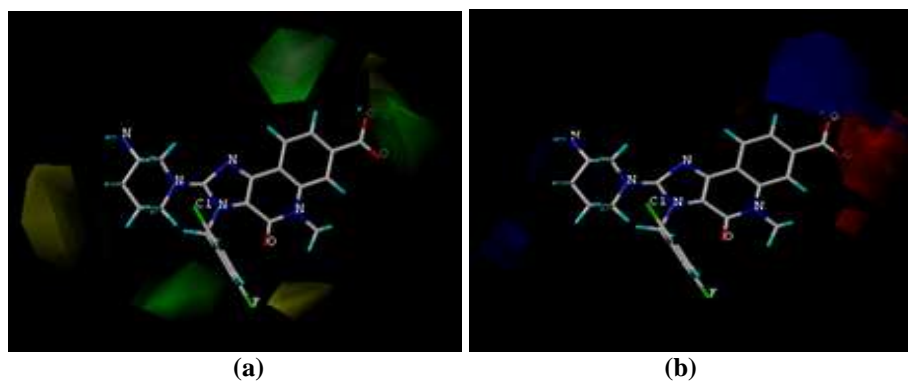


Figure 6: CoMFA contour maps for Pullman charge (of Compound 28, Table 7)

(a) Steric contributions, (b) Electrostatic contributions.



Figure 7: CoMFA contour maps for Fromal charge (of Compound 28, Table 7)

(a) Steric contributions, (b) Electrostatic contributions.

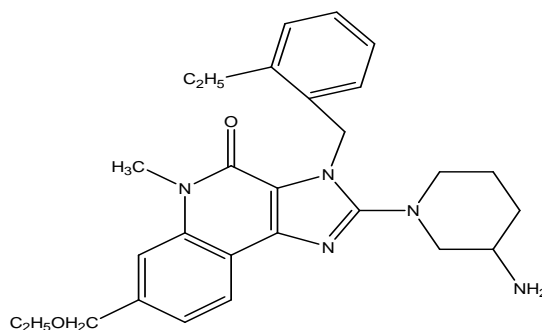


Figure 8: CoMFA contour maps for MMFF94 charge (of Compound 28, Table 7)  
(a) Steric contributions, (b) Electrostatic contributions.

### C. Docking

The DPP-IV structure was utilized in subsequent docking experiments without energy minimization. Potency of compounds is determined on the basis of their docking scores or interaction energies. One compound out of 8 compounds designed formed active interaction with the protein receptor (PDB code: 4DSA) namely compound

1-8. The most potent imidazoquinoline compound 5(2-(-Amino-piperidin-1yl)-7-ethoxymethyl-3-(2-ethyl-benzyl)-5-methyl-3,5-dihydro-imidazo[4,5-c]quinolin-4-one) was selected according to its docking scores 6.4314. The key residues and hydrogen bonds were labeled. The hydrogen bonds are shown by yellow color broken lines in fig. 10.



2-(-Amino-piperidin-1yl)-7-ethoxymethyl-3-(2-ethyl-benzyl)-5-methyl-3,5-dihydro-imidazo[4,5-c]quinolin-4-one (Compound 5)

Table 14: The Docking Results to DPP-IV Receptor.

S.no	Name	Total score	Crash	Polar
1	2-(-Amino-piperidin-1yl)-7-ethoxymethyl-3-(2-ethyl-benzyl)-5-methyl-3,5-dihydro-imidazo[4,5-c] quinolin-4-one	6.4314	-1.8422	2.0116

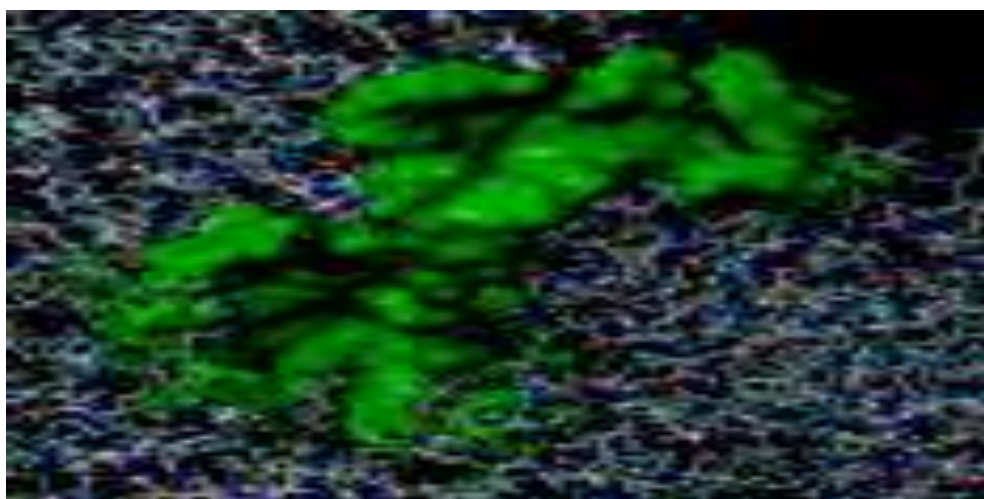
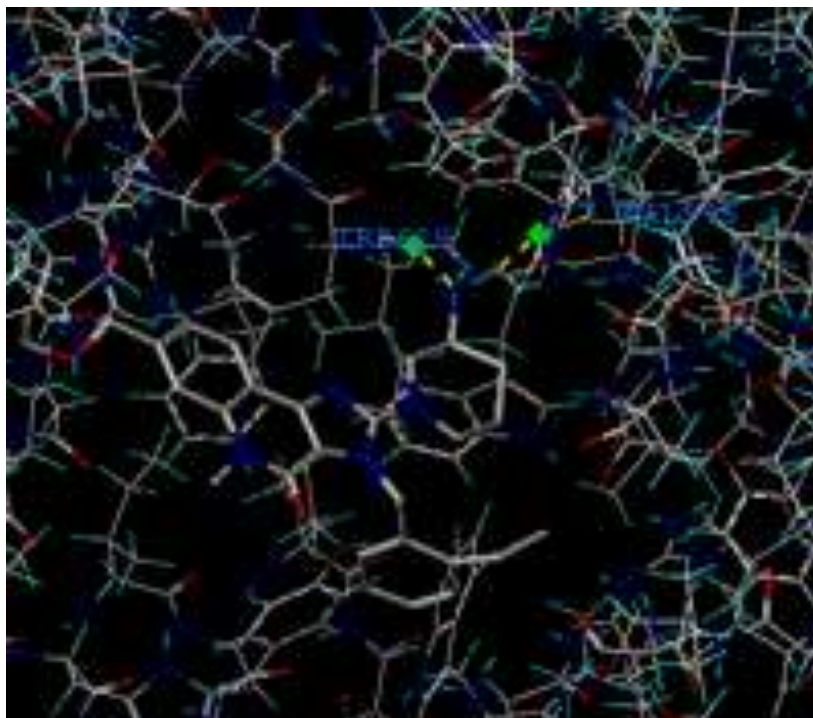


Figure 9: Protomol Structure for DPP-IV receptor (4DSA pdb.).



**Figure 10: Binding mode between compound 5 and active site of DPP-IV (PDB code 4DSA). The receptor is showed hydrogen bonding interaction, in which Val546 and Trp629 residues are depicted in blue.**

#### 4. CONCLUSION

The present study successfully applied pharmacophore mapping, 3D-QSAR and molecular docking analysis to characterize a set of synthesized DPP-IV inhibitors. A series of imidazoquinoline derivatives were taken from the literature for the pharmacophore and CoMFA studies. The selected series of imidazoquinoline derivatives included 47 compounds out of which 38 compounds were put in training set and remaining 9 compound were put in test set on the basis of diversity using the SYBYL X 2.1.1 software. The optimal pharmacophore model contains nine pharmacophore features. The models include four hydrophobes, three hydrogen bond acceptors and two positive nitrogen centres. The CoMFA models generated both exhibited reliable correlative and predictive abilities. Successful CoMFA models were generated from imidazoquinoline derivatives which displayed a cross-validated correlation coefficient ( $Q^2$ ) of 0.526 and a non-cross related coefficient ( $R^2$ ) of 0.946. Moreover the contour maps derived from CoMFA models provided enough information to understand the SAR and to identify the structural features influencing DPP-IV inhibitory activity. On the basis of pharmacophoric features obtained by pharmacophore modeling and steric and electrostatic contributions obtained from CoMFA studies eight compounds were designed. The docking studies of these eight designed compounds were performed using the SURFLEX DOCK module of SYBYL X 2.1.1 software. The binding mode of designed compounds at the active site of DPP-IV enzyme (PDB ID. 4DSA) was explored and hydrogen-bonding interactions were observed between the inhibitor and the target. Docking view of the most active compound from the designed compound demonstrated

the interaction with Val-546 and Trp-629 of 4DSA receptor. The information obtained by the detailed molecular modeling study provides a methodology for predicting the affinity of imidazoquinoline derivatives for guiding structural design of novel potent DPP-IV inhibitors. The study will serve as a useful guideline for designing the novel compounds with significant DPP-IV inhibitory activity.

#### 5. REFERENCES

1. J. Shoback, *et al.*, Greenspan's basic & clinical endocrinology, McGraw-Hill Medical, New York, 9<sup>th</sup> edition, 2011; 145-148.
2. S.H. Saydah, *et al.*, Post challenge hyperglycemia and mortality in a national sample of U.S. adults, *Diabetes Care*, 2001; 24(8): 1397-402.
3. P. Danaei, *et al.*, National, regional, and global trends in fasting plasma glucose and diabetes prevalence since 1980: systematic analysis of health examination surveys and epidemiological studies with 370 country-years and 2.7 million participants. *Lancet*, 2011; 31-40.
4. W. L. Bennett, *et al.*, Comparative effectiveness and safety of medications for type 2 diabetes: An update including new drugs and 2-drug combinations, *Annals of internal medicine*, 2011; 154(9): 602-613.
5. L.L. Baggio, D.J. Drucker, Biology of incretins: GLP-1 and GIP, *Gastroenterology*, 2007; 132: 2131-2157.
6. R.A. DeFronzo, *et al.*, Pathogenesis of NIDDM: a balanced overview, *Diabetes Care*, 1992; 15: 318-368.
7. B.D. Green, *et al.*, Dipeptidyl peptidase IV (DPP IV) inhibitors: a newly emerging drug class for the

- treatment of type 2 diabetes, *Diabetes and Vascular Disease Research*, 2006; 3: 159–165.
8. G.A. Herman, *et al.*, Effect of single oral doses dipeptidyl peptidase-4 inhibitor, on incretin and plasma glucose levels after an oral glucose tolerance test in patients with type 2 diabetes, *The Journal of Clinical Endocrinology and Metabolism*, 2006; 91: 4612–4619.
  9. Y. Ikuma, *et al.*, Discovery of 3H-imidazo [4, 5-c] quinolin-4(5H)-ones as potent and selective dipeptidyl peptidase IV (DPP-IV) inhibitors, *Bioorganic & Medicinal Chemistry*, 2012; 20: 5864–5883.
  10. H. Zhong and J.P. Bowen, SYBYL for drug discovery, *Journal of Americal Chemical Society*, 2007; 129: 5780.
  11. S.Y. Yang, Pharmacophore modeling and applications in drug discovery: challenges and recent advances, *Drug discovery today*, 2010; 15(11-12): 444-450.
  12. G. Kothandan, *et al.*, A combined 3D QSAR and pharmacophore-based virtual screening for the identification of potent p38 MAP kinase inhibitors: an in silico approach, *Medicinal Chemistry Research*, 1-15.